Monatsh Chem (2011) 142:1097–1104
DOI 10.1007/s00706-011-0547-x

ORIGINAL PAPER

NMR and NQR parameters of Si-doped (6,0) *zigzag* single-walled boron phosphide nanotubes: a density functional study

Mohammad T. Baei · Ali Varasteh Moradi · Parviz Torabi · Masoumeh Moghimi

Received: 29 March 2011 / Accepted: 30 May 2011 / Published online: 28 June 2011

Abstract Electronic structure properties including bond lengths, bond angles, tip diameters, dipole moments, energies, band gaps, and nuclear magnetic resonance (NMR) and nuclear quadrupole resonance (NQR) parameters were calculated using density functional theory (DFT) for Si-doped boron phosphide nanotubes (BPNTs). Geometry optimizations were carried out at the B3LYP/6-31G* level of theory using the Gaussian 03 program suite. The chemical shielding parameters for the sites of various ^{29}Si, ^{11}B, and ^{31}P atoms, and quadrupole coupling constants and asymmetry parameters at the sites of various ^{11}B nuclei, were calculated for the Si-doped (6,0) *zigzag* BPNT models. The dipole moments and average B–P bond lengths of the Si-doped BPNT structures show slight changes between the Si-doped and pristine models. For the Si_B model the diameter values are increased, whereas in the Si_P model the changes of the diameter values are negligible. In comparison with the pristine model, the band gaps of the Si_B and Si_P models are reduced, whereas their electrical conductance is increased. Comparison of the NMR and NQR parameters calculated for the Si_B and Si_P models showed that the electronic structure properties of the Si_B (6,0) *zigzag* BPNT model are more strongly influenced than those of the Si_P model.

Keywords Boron phosphide nanotubes · Silicon · NMR · NQR · DFT

M. T. Baei (✉)
Department of Chemistry, Azadshahr Branch, Islamic Azad University, Azadshahr, Golestan, Iran
e-mail: Baei52@yahoo.com

A. V. Moradi
Department of Chemistry, Gorgan Branch, Islamic Azad University, Gorgan, Iran

P. Torabi
Department of Chemistry, Mahshahr Branch, Islamic Azad University, Mahshahr, Iran

M. Moghimi
Department of Chemistry, Gonbad Kavoos Branch, Islamic Azad University, Gonbad Kavoos, Golestan, Iran

Introduction

Since the synthesis of carbon nanotubes (CNTs) by Ijima [1], single-walled carbon nanotubes (SWCNTs) have attracted great interest owing to their physical and chemical properties [1–3] and applications as novel materials [4, 5]. The electronic properties of CNTs depend on their diameter and chirality. Many investigations have been undertaken to investigate non-carbon-based nanotubes, which exhibit electronic properties independent of these parameters. Among such nanotubes, use of group III and V elements, which are the neighbors of C in the Periodic Table, has been an interesting subject of many studies, using materials such as boron nitride (BN) [6], aluminum nitride (AlN) [7], gallium nitride (GaN) [8], indium nitride (InN) [9], boron phosphide (BP) [10], aluminum phosphide (AlP) [11], gallium phosphide (GaP) [12], and indium phosphide (InP) [13]. These nanotubes are inorganic analogs of carbon nanotubes (CNTs) and have good physical properties for a broad variety of applications; such nanotubes are always semiconductors [14]. Also, such nanotubes are being considered as materials that are more appropriate than CNTs for application in specific electronic and mechanical devices. However, the properties of nitride compounds have been studied more often than the properties of phosphide compounds [15, 16], and further study

of the electronic properties of BPNTs is necessary. Nuclear magnetic resonance (NMR) spectroscopy is one of the best techniques to study the electronic structure properties of materials [17]. Moreover, doping of BPNTs by Si atoms may be able to yield changes in the interactions between the nanotube and foreign atoms or molecules. Therefore, the objective of the present work is to study the electronic structure properties of Si-doped BPNTs by performing density functional theory (DFT) calculations of the NMR and NQR parameters of representative (6,0) *zigzag* BPNT models (Fig. 1). The electronic structure properties, including bond lengths, bond angles, tip diameters, dipole moments (μ), energies, band gaps, and NMR and NQR parameters in the pristine and two Si-doped BPNT structures, were investigated by calculations of the chemical shift (CS) tensors at the sites of various ^{29}Si, ^{11}B, and ^{31}P atoms, and NQR calculations at the sites of ^{11}B atoms.

Results and discussion

Structures of the BPNTs

The structural properties, consisting of the B–P bond lengths, bond angles, tip diameters, dipole moments (μ), energies, and band gaps for the investigated models of the (6,0) *zigzag* BPNTs, are summarized in Table 1. There are two forms of Si-doped BPNT for the (6,0) *zigzag* model, namely with the Si atom doped at a B site (Si_B model, Fig. 1a) or at a P site (Si_P model, Fig. 1b). There are B–P and Si–P bonds in the Si_B model and B–P and B–Si bonds in the Si_P model. In Fig. 1, the atoms of the BPNTs are numbered in order to describe the relevant structural parameters. The calculated results showed that the average B–P bond lengths are almost the same in the investigated (6,0) *zigzag* BPNT models. In Fig. 1a and b, the Si–P and Si–B bond lengths are the largest among the investigated (6,0) *zigzag* BPNT models. Compared with the pristine model, the Si atom relaxes out of the nanotube surface in Fig. 1a and b. The distances between the Si atom and the P14, P8, and P9 atoms in Fig. 1a are 2.216 and 2.250 Å, and the distances between the Si atom and the B3, B8, and B9 atoms in Fig. 1b are 1.983 and 1.970 Å (Table 1). The P8–Si–P9 and P8–Si–P14 bond angles in Fig. 1a are 119.2° and 114.0°, and the B3–Si–B8 and B8–Si–B9 bond angles in Fig. 1b are 117.4° and 107.3°, indicating some structural deformation. Furthermore, in the pristine model, it should be noted that B atoms relax in, while P atoms relax out, with respect to the nanotube surface, yielding different diameters of 5.84 Å for the B mouth and 6.66 Å for the P mouth, whereas in the Si_B model (Fig. 1a), the diameters at the B and P terminals undergo changes to 5.95 and 7.13 Å, and in the Si_P model (Fig. 1b) the diameters at the B and P terminals undergo changes to 5.86 and 6.67 Å. For the Si_B model (Fig. 1a) the diameter values are increased, whereas in the Si_P model (Fig. 1b) the changes of the diameters were negligible. It must be noted that significant changes of geometry are limited to atoms located in the immediate neighborhood of the Si atom, whereas those of other atoms remain almost unchanged. Also, the calculated energy value for the Si_B model (Fig. 1a) is higher than that for the Si_P model (Fig. 1b). We studied the influence of Si-doping on the electronic properties of the BPNTs. The total density of states (DOS) of these tubes are shown in Fig. 2. As is

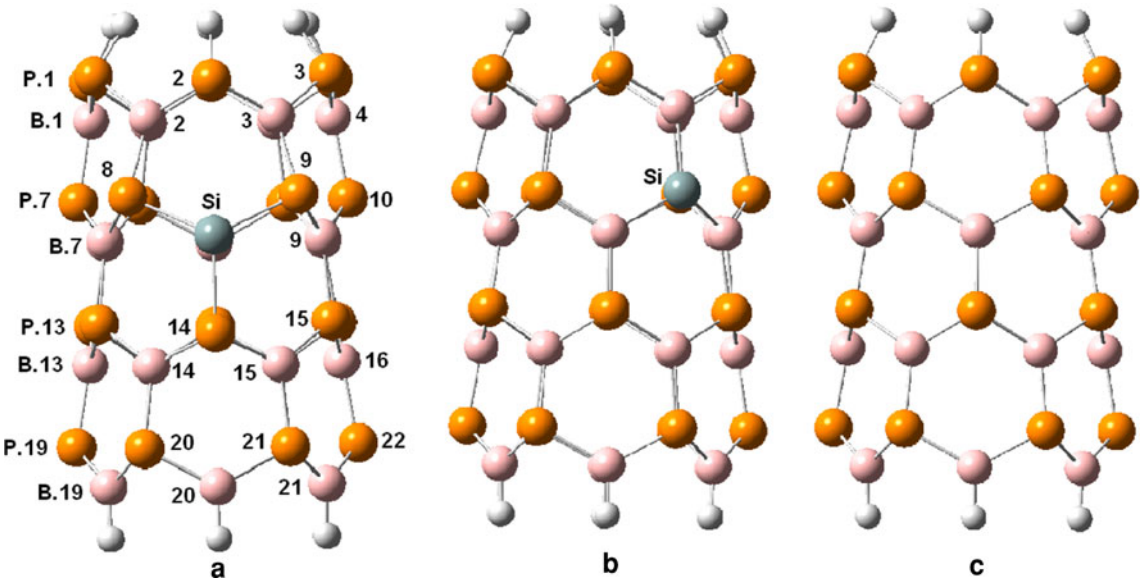

Fig. 1 **a**, **b** Two-dimensional (2D) views of the Si-doped (6,0) *zigzag* BPNTs in the Si_B and Si_P models. **c** 2D views of the pristine (6,0) *zigzag* BPNT

Table 1 Structural properties of representative (6,0) *zigzag* BPNT models

Property Bond length/Å	Fig. 1a	Fig. 1b	Fig. 1c	Property Bond length/Å	Fig. 1a	Fig. 1b	Fig. 1c
P1–6–H	1.418	1.418	1.418	B14–P20	1.906	1.898	1.899
B19–24–H	1.190	1.190	1.190	B15–P21	1.906	1.898	1.899
P1–B1	1.900	1.904	1.904	B16–P22	1.896	1.898	1.899
P1–B2	1.897	1.904	1.904	P19–B19	1.878	1.885	1.885
P2–B2	1.924	1.913	1.904	P20–B19	1.882	1.885	1.885
P2–B3	1.924	1.892	1.904	P20–B20	1.889	1.886	1.885
P3–B3	1.897	1.892	1.904	P21–B20	1.889	1.884	1.885
P3–B4	1.900	1.913	1.904	P21–B21	1.882	1.884	1.885
B1–P7	1.889	1.894	1.894	P22–B21	1.878	1.886	1.885
B2–P8	1.901	1.904	1.894	Average	1.898	1.896	1.897
B3–P9	1.901	–	1.894	Si–P14	2.216	–	–
B4–P10	1.889	1.904	1.894	Si–P8 and P9	2.250	–	–
P7–B7	1.889	1.905	1.903	Si–B3	–	1.983	–
P8–B7	1.912	1.898	1.903	Si–B8 and 9	–	1.970	–
P8–B8	–	1.889	1.903	Bond angles/°			
P9–B8	–	–	1.903	P1–B2–P2	121.9	120.0	121.7
P9–B9	1.912	–	1.903	B2–P2–B3	99.9	101.6	101.1
P10–B9	1.889	1.889	1.903	P7–B7–P8	120.9	122.0	122.1
B7–P13	1.892	1.893	1.891	P8–B8–P9	–	–	122.1
B8–P14	–	1.875	1.891	B3–Si–B8	–	117.4	–
B9–P15	1.892	1.875	1.891	B8–Si–B9	–	107.3	–
P13–B13	1.896	1.904	1.902	P8–Si–P9	119.2	–	–
P13–B14	1.895	1.904	1.902	P8–Si–P14	114.0	–	–
P14–B14	1.926	1.902	1.902	Diameter (B–tip)/Å	5.95	5.86	5.84
P14–B15	1.926	1.909	1.902	Diameter (P–tip)/Å	7.13	6.67	6.66
P15–B15	1.895	1.909	1.902	μ/Debye	2.10	2.29	2.07
P15–B16	1.896	1.902	1.902	Energy/keV	−246.572	−237.958	−239.372
B13–P19	1.896	1.899	1.899	Band gap/eV	$\alpha = 1.88$	$\alpha = 1.80$	2.27
					$\beta = 2.22$	$\beta = 1.97$	

Data for the pristine model are from Ref. [18]

evident from Fig. 2, the calculated band gap of the perfect (6,0) *zigzag* single-walled BPNT is 2.27 eV [18], whereas the calculated band gaps of the Si_B model (Fig. 1a) and the Si_P model (Fig. 1b) for α and β molecular orbitals are 1.88, 2.22 and 1.80, 1.97 eV. The total density of states (TDOS) of these tubes show significant changes due to Si-doping in the gap regions of the TDOS plots.

Also, the band gaps showed differences between the two forms (Fig. 1a, b). In comparison with the pristine model, the band gaps of the models shown in Fig. 1a and b were reduced while their electrical conductance was increased, with the doping in the Si_P model having a stronger effect than the doping in the Si_B model on the band gap of the BPNT (Table 1). The dipole moments (μ) of the Si-doped BPNT structures (Fig. 1a, b) showed slight changes due to the Si-doping with respect to the pristine model. Also, the dipole moment (μ) for the model shown in Fig. 1b was somewhat different from that of the model shown in Fig. 1a.

NMR parameters of the (6,0) zigzag BPNTs

The NMR parameters for the investigated (6,0) *zigzag* BPNT models are summarized in Table 2. In the model of the pristine (6,0) *zigzag* BPNT, there are 24 B and 24 P atoms and the NMR parameters are separated into four layers: 1–6, 7–12, 13–18, and 19–24 (Table 2, Fig. 1c) [18]. In the model, the values of the NMR parameters of each group were the same; however, the results in Table 2 show that the calculated NMR parameters were not similar for different groups, meaning that the CS parameters for the atoms of each layer have equivalent chemical environment and electrostatic properties. Atoms B1 to B6 and P19 to P24, which are located near the P- and B-terminated

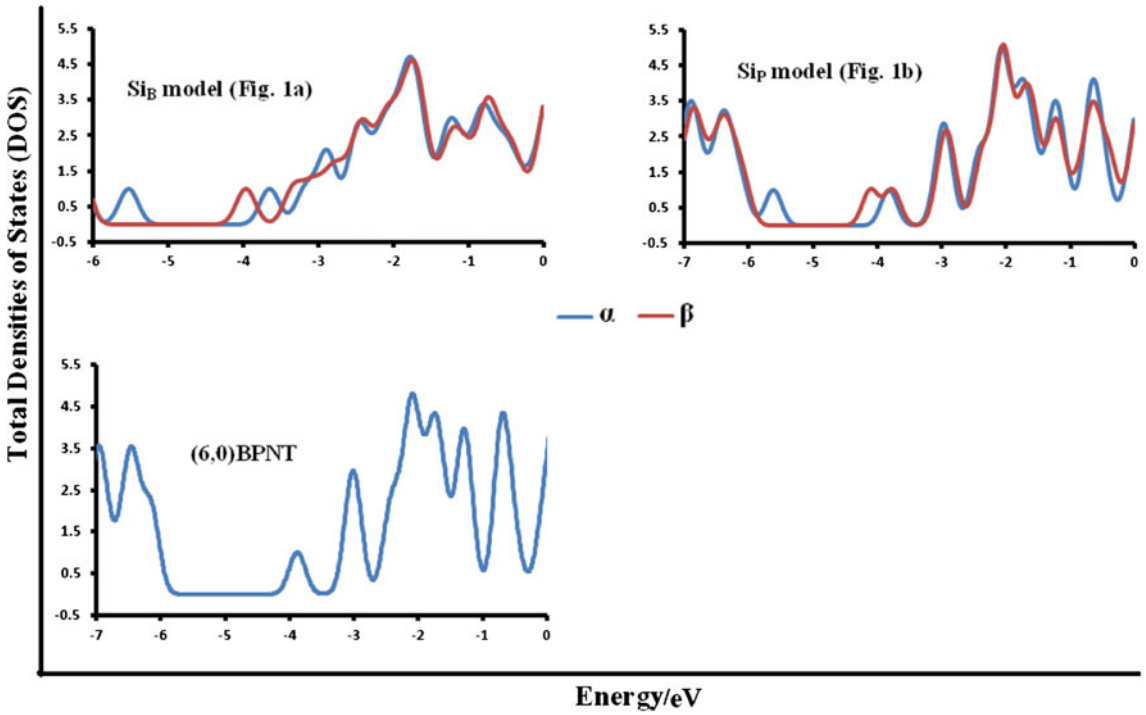

Fig. 2 Total density of states (DOS) for different BPNT models

ends, have the smallest values of the CS^I parameters but the largest values of the CS^A parameters among the B and P atoms in the model of the pristine (6,0) *zigzag* BPNT. Atoms B19 to B24 and P1 to P6, which are located at the edge of the (6,0) *zigzag* BPNT (B- and P-terminated ends), have the largest values of the CS^I parameters, but the values of the CS^A parameters of the layer were not the smallest values among the B and P atoms. Therefore, from one end (P-terminated end) to the other end of the nanotube (B-terminated end), the NMR parameters show some changes. In Fig. 1a, i.e., the Si_B model, atom B8 is doped by the Si atom, which results in a Si–P bond. The calculated results in Table 2 show that, among the B atoms of the model shown in Fig. 1a, i.e., Si_B, for atoms B19 to B24 located at the edge of the (6,0) *zigzag* BPNT (B-terminated ends), the changes of the CS^I and CS^A values of the B atoms are negligible. For atoms B1 to B6, which are located near the P-terminated end, the CS^I and CS^A values of the B1 and B4 atoms show some significant changes due to the Si-doping; the CS^I values of the atoms are increased, whereas the CS^A values of the atoms are decreased. However, other B atoms of this group show no significant change due to the Si-doping of the (6,0) *zigzag* BPNT. For atoms B7 to B12, in this group, the B8 atom is doped by the Si atom. Therefore, the CS^I and CS^A values of the B7 and B9 atoms that are bonded indirectly to the Si atom show the most significant changes due to the Si-doping among the B atoms of the (6,0) *zigzag* BPNT; the CS^I values of the atoms are increased, whereas the CS^A values of the atoms are decreased. However, the changes in the values of the CS parameters for atoms B10 and B12, which are indirectly bonded to the Si atom, are also notable, whereas the CS^I value of atom B11 remained almost unchanged. For atoms B13 to B18, the CS^A parameters do not exhibit any significant changes due to the Si-doping in the (6,0) *zigzag* BPNT, but the CS^I value of atoms B13, B16, B17, and B18 are influenced by the Si-doping. The P atom has a lone pair of electrons in the valence shell, therefore there are differences between the electronic structure properties of B and P atoms. Among the P atoms of the model shown in Fig. 1a, i.e., the Si_B model, atoms P8, P9, and P14 are directly bonded to the Si atom. The calculated results in Table 2 show that atoms P1 to P6, which are located at the edge of the (6,0) *zigzag* BPNT (P-terminated ends), show significant changes due to the Si-doping, unlike the B atoms in the Si_B model shown in Fig. 1a. For atoms P1, P2, P3, and P5, the CS^A values of the atoms show significant changes due to the Si-doping, but the CS^I values of the atoms change only slightly. For atoms P7 to P12, the CS^I and CS^A values of atoms P8 and P9, which are directly bonded to the Si atom, show the most significant changes due to the Si-doping among the P atoms of the (6,0) *zigzag* BPNT; the CS^I values of the atoms are increased, whereas the CS^A values of the atoms are decreased. The changes of the CS^A values of atoms P7, P10, P11, and P12 are negligible. However, the CS^I values of the atoms change

Table 2 NMR parameters (ppm) of representative (6,0) *zigzag* BPNT models for sites of various ^{29}Si, ^{11}B, and ^{31}P atoms

Nucleus	Fig. 1a		Fig. 1b		Fig. 1c		Nucleus	Fig. 1a		Fig. 1b		Fig. 1c	
	CS^I	CS^A	CS^I	CS^A	CS^I	CS^A		CS^I	CS^A	CS^I	CS^A	CS^I	CS^A
B1	24.9	131.2	18.5	143.2	17.9	143.9	P1	372.6	141.4	377.3	116.8	383.0	115.0
B2	20.9	147.3	23.7	142.5	17.9	143.9	P2	395.6	72.4	375.0	116.8	383.0	115.0
B3	20.9	147.3	26.2	167.1	17.9	143.9	P3	372.6	141.4	375.0	116.8	383.0	115.0
B4	24.9	131.2	23.7	142.5	17.9	143.9	P4	387.4	114.6	377.3	116.8	383.0	115.0
B5	16.4	145.2	18.5	143.2	17.9	143.9	P5	376.6	96.7	380.1	119.7	383.0	115.0
B6	16.4	145.2	18.5	143.2	17.9	143.9	P6	387.4	114.6	380.1	119.7	383.0	115.0
B7	45.7	99.9	34.0	117.5	30.7	115.8	P7	360.6	253.1	375.2	250.2	373.9	250.0
B8	–	–	31.2	140.4	30.7	115.8	P8	408.1	151.6	338.8	278.0	373.9	250.0
B9	45.7	99.9	31.2	140.4	30.7	115.8	P9	408.1	151.6	–	–	373.9	250.0
B10	39.2	110.0	34.0	117.5	30.7	115.8	P10	360.6	253.1	338.8	278.0	373.9	250.0
B11	31.1	110.1	30.0	117.6	30.7	115.8	P11	384.1	254.7	375.2	250.2	373.9	250.0
B12	39.2	110.0	30.0	117.6	30.7	115.8	P12	384.1	254.7	372.7	249.9	373.9	250.0
B13	34.6	115.5	25.9	116.2	25.1	117.4	P13	333.9	256.5	338.0	251.0	341.0	247.7
B14	24.0	116.8	26.0	115.3	25.1	117.4	P14	394.0	241.9	336.6	265.4	341.0	247.7
B15	24.0	116.8	28.1	117.5	25.1	117.4	P15	333.9	256.5	336.6	265.4	341.0	247.7
B16	34.6	115.5	26.0	115.3	25.1	117.4	P16	335.8	256.9	338.0	251.0	341.0	247.7
B17	21.9	117.8	25.9	116.2	25.1	117.4	P17	344.7	243.0	338.6	252.7	341.0	247.7
B18	21.9	117.8	26.0	117.8	25.1	117.4	P18	335.8	256.9	338.6	252.7	341.0	247.7
B19	43.1	127.2	39.6	127.4	39.7	126.4	P19	326.8	288.2	332.1	275.4	333.7	274.5
B20	38.7	121.3	40.3	126.0	39.7	126.4	P20	329.1	263.3	335.5	274.5	333.7	274.5
B21	43.1	127.2	40.3	126.0	39.7	126.4	P21	329.1	263.3	325.5	277.5	333.7	274.5
B22	40.1	126.0	39.6	127.4	39.7	126.4	P22	326.8	288.2	335.5	274.5	333.7	274.5
B23	39.2	125.9	39.6	126.6	39.7	126.4	P23	335.8	271.5	332.2	275.4	333.7	274.5
B24	40.1	126.0	39.6	126.5	39.7	126.4	P24	335.8	271.5	333.8	276.1	333.7	274.5
Si	270.3	198.6	257.0	291.7	–	–	–	–	–	–	–	–	–

Data for the pristine model are from Ref. [18]

slightly. Among atoms P13 to P18, only the CS^I value of atom P14, which is directly bonded to the Si atom, showed significant changes due to the Si-doping, whereas the CS parameters of the other P atoms of this group changed only slightly. For atoms P19 to P24, which are located near the B-terminated end, the CS^I and CS^A values of atoms P19, P20, P21, and P22 showed some significant changes due to the Si-doping, whereas the CS parameters of P23 and P24 remained almost unchanged.

In Fig. 1b, i.e., the Si_P model, atom P9 is doped by a Si atom, from which a Si–B bond results, and atoms B8, B9, and B3 are directly bonded to the Si atom. The calculated results in Table 2 show that, among the B atoms of Fig. 1b (Si_P model), for atoms B19 to B24, which reside at the edge of the (6,0) *zigzag* BPNT (B-terminated ends), the changes of the CS^I and CS^A values of the B atoms are negligible. For atoms B1 to B6, which are located near the P-terminated end, the CS^I and CS^A values of atom B3, which is directly bonded to the Si atom, and the CS^I values of atoms B2 and B4 show significant changes due to the Si-doping, with the CS^I and CS^A values of the atoms being increased. However, other B atoms of this group do not exhibit any significant changes due to the Si-doping in the (6,0) *zigzag* BPNT. For atoms B7 to B12, the CS^A values of atoms B8 and B9, which are directly bonded to the Si atom, show the most significant changes due to the Si-doping among the B atoms of the group; the CS^A values of the atoms are increased, whereas the CS^I values of the atoms remain almost unchanged. However, the CS^I values for atoms B7 and B10, which are indirectly bonded to the Si atom, change only slightly. The CS parameters of the other B atoms of this group remain almost unchanged. For atoms B13 to B18, the CS parameters do not exhibit any significant changes due to the Si-doping in the (6,0) *zigzag* BPNT. For the P atoms of Fig. 1b, i.e., the Si_P model, the calculated results in Table 2 show that, for atoms P1 to P6, which reside at the edge of the (6,0) *zigzag* BPNT (P-terminated ends), the changes of the CS^I and CS^A values due to the Si-doping are negligible, unlike the P atoms of Fig. 1a, i.e., the Si_B model, which show significant changes

due to the Si-doping. For atoms P7 to P12, in this group, the P9 atom is doped by the Si atom and the CS^I and CS^A values of atoms P8 and P10, which are indirectly bonded to the Si atom, show the most significant changes due to the Si-doping among the P atoms of the (6,0) *zigzag* BPNT; the CS^I values of the atoms are decreased, whereas the CS^A values of the atoms are increased. For the other P atoms of Fig. 1b, i.e., the Si_P model, the changes of the CS^I and CS^A values of the P atoms are negligible. The values of the NMR parameters (CS^I and CS^A) of the ^{29}Si atom in the Si-doped (6,0) *zigzag* BPNTs are summarized in Table 2. The results of Table 2 show that the values of the CS^I parameters of the ^{29}Si atom in Fig. 1a, i.e., the Si_B model, are larger than in Fig. 1b, i.e., the Si_P model, whereas the values of the CS^A parameters of Fig. 1b, i.e., the Si_P model, are larger than in Fig. 1a, i.e., the Si_B model of the (6,0) *zigzag* BPNT. Comparison of the NMR parameters calculated for the models shown in Figs.1a and b shows that the properties of the electronic structure of Fig. 1a of the Si-doped (6,0) *zigzag* BPNT where a B atom is doped by the Si atom (Si_B model) are more strongly influenced than those of Fig. 1b where a P atom is doped by the Si atom (Si_P model).

^{11}B electric field gradient tensors of the (6,0) zigzag models

The NQR parameters at the sites of various ^{11}B nuclei for the optimized investigated (6,0) *zigzag* BPNT models are summarized in Table 3. There are 24 B atoms in the considered (6,0) *zigzag* models, and the NQR parameters are separated into four layers based on the similarity of the calculated electric field gradient (EFG) tensors in each layer. The results in Table 3 show that the calculated NQR parameters are not similar for various nuclei; hence, the electrostatic environment of the BPNT is not equivalent throughout the length of the nanotube models. In Fig. 1, atom B19 indicates the position of the first layer, atom B13 indicates the position of the second layer, atom B7 indicates the position of the third layer, and atom B1 indicates the position of the fourth layer in the considered *zigzag* models. The B19 layer is placed at the end of the tubes and includes B atoms. In the (6,0) *zigzag* models, the values of $C_Q(^{11}B19)$ are the largest among the ^{11}B nuclei (Table 3), indicating greater orientation of the EFG tensor eigenvalues along the *z*-axis of the electronic distribution at the sites of the $^{11}B19$ nuclei. The electrostatic environment of atom B19 is stronger than in the other layers along the length of the tube. Other research has shown that such nanotubes grow from their ends; hence, the properties of the end nuclei in nanotubes are important for their growth and synthesis [19, 20]. Therefore, in the BPNTs the B atoms located at the edge of the (6,0) *zigzag* nanotubes play important roles in determining the electronic behavior of the (6,0) *zigzag* BPNTs, because the geometrical properties of this layer are different from the other layers. The B13 layer is located at the second layer in the considered (6,0) *zigzag* BPNT models. The values of $C_Q(^{11}B)$ and η_Q are significantly reduced (Table 3). In the first layer of the pristine model, the B–P bond distances are 1.885 Å (B19-P19), but in the second layer the B–P bond distances are 1.902 Å (B13-P13). Therefore, the significant difference between the NQR parameters of the first layer and the other layers are due to the change of the geometrical parameters. The B7 layer is located at the third layer in the considered (6,0) *zigzag* BPNT models. The values of $C_Q(^{11}B)$ of the models increased slightly, whereas the values of η_Q of the models were slightly reduced. For the B1 layer, which is located near the P-terminated end, the values of $C_Q(^{11}B)$ and η_Q significantly increased except for the value of $C_Q(^{11}B)$ for Fig. 1a, i.e., the Si_B model, which remained unchanged. Comparison of the calculated $C_Q(^{11}B)$ parameters of the considered (6,0) *zigzag* BPNT models shows that the electronic sites of the B atoms of the B19 layer (first layer) in Fig. 1a, i.e., the Si_B model, exhibit greater changes than the Si_P model in Fig. 1b with respect to the pristine model. In the B13 layer (second layer), the electronic sites of the B atoms in Fig. 1a, i.e., the Si_B model, changed significantly compared with the pristine model, whereas the electronic sites of the B atoms in Fig. 1b, i.e., the Si_P model, remained unchanged with respect to the pristine model. The changes of the electronic sites of the B atoms of the third layer (B7 layer) are similar for the two Si-doped BPNT models. However, the electronic sites of the B atoms of the fourth layer (B1 layer) in Fig. 1a, i.e., the Si_B model, show significant changes compared with the pristine model, whereas the electronic sites of the B atoms in Fig. 1b, i.e., the Si_P model, in the layer remained unchanged. Finally, the average values of $C_Q(^{11}B)$ and η_Q for Fig. 1a, i.e., the Si_B (6,0) *zigzag* BPNT model, are greater than those for Fig. 1b, i.e., the Si_P model, and the pristine (6,0) *zigzag* BPNT model, because the BPNT is significantly influenced by the Si-doping. Therefore, the electronic sites of the B atoms in Fig. 1a, i.e., the Si_B

Table 3 The ^{11}B NQR parameters

Nucleus	Fig. 1a		Fig. 1b		Fig. 1c	
	C_Q/MHz	η_Q	C_Q/MHz	η_Q	C_Q/MHz	η_Q
B19	3.74	0.38	3.64	0.42	3.62	0.41
B13	3.26	0.16	3.02	0.06	3.02	0.05
B7	3.28	0.09	3.28	0.03	3.16	0.00
B1	3.28	0.12	3.33	0.11	3.32	0.12
Average	3.39	0.19	3.32	0.16	3.28	0.14

Data for the pristine model are from Ref. [18]

model, exhibit greater changes than in Fig. 1b, i.e., the Si_P model. This trend is in agreement with the change in the NMR parameters of Fig. 1a, i.e., the Si_B model, in comparison with the model of the pristine (6,0) *zigzag* BPNT.

Conclusions

We studied the electronic structure properties including bond lengths, bond angles, tip diameters, dipole moments (μ), energies, band gaps, and NMR and NQR parameters of pristine and Si-doped BPNTs by means of DFT calculations. The calculated results showed that average values of the B–P bond lengths are almost the same in the investigated (6,0) *zigzag* BPNT models. For the Si_B model (Fig. 1a) the diameters are increased, whereas in the Si_P model (Fig. 1b) the changes of the diameter values were negligible. The dipole moments (μ) of the Si-doped BPNT structures (Fig. 1a and b) show minor changes due to the Si-doping with respect to the pristine model. In comparison with the pristine model, the band gaps of the models shown in Figs.1a and b are reduced, whereas their electrical conductance is increased. The NMR parameters for the pristine model are separated into four layers, and the NMR values for the ^{11}B and ^{31}P atoms that are directly bonded to the Si atom in the Si-doped models are significantly changed. Comparison of the calculated NMR parameters in the Si_B and Si_P models shows that the properties of the electronic structure of the Si_B model (Fig. 1a) of the (6,0) *zigzag* BPNTs are more strongly influenced than those of the Si_P model (Fig. 1b). The NQR values of the first layers belonging to those B atoms located at the edges of the BPNTs were higher than those of the other layers along the length of the tube, showing the dominant role of these B atoms in determining the electronic behavior of the BPNT. The electronic sites of the B atoms in the Si_B model (Fig. 1a) of the (6,0) *zigzag* BPNTs showed greater changes than for the Si_P model (Fig. 1b). The NMR and NQR results show that the Si_B model is a more reactive material than either the pristine or the Si_P model of the (6,0) *zigzag* BPNTs.

Methods

In the present work, the electronic structure properties of BPNTs were studied by using representative models of (6,0) *zigzag* BPNTs with the nanotube ends saturated by hydrogen atoms. Each of the representative models has three forms (Fig. 1), namely pristine (Fig. 1c), or with a B atom doped by a Si atom, i.e., the Si_B model (Fig. 1a), or with a P atom doped by a Si atom, i.e., the Si_P model (Fig. 1b). We investigated the influence of the Si-doping on the properties of the (6,0) *zigzag* single-walled BPNT. The hydrogenated models of the pristine (6,0) *zigzag* BPNTs and the two Si-doped BPNT models consisted of 60 atoms with formulas $B_{24}P_{24}H_{12}$ (pristine), $B_{23}P_{24}H_{12}Si$ (Si_B model), and $B_{24}P_{23}H_{12}Si$ (Si_P model). In the first step, all the atomic geometrical parameters of the structures were allowed to relax in the optimization at the DFT level of B3LYP exchange functional and 6-31G* standard basis set. Then, the CS tensors of the sites of various ^{29}Si, ^{11}B, and ^{31}P atoms and NQR parameters of ^{11}B were calculated for the optimized structures at the B3LYP/6-31G* level. It is noted that, when applying DFT, the B3LYP level usually gives more reliable results in comparison with experiments and is usually more convincing [21, 22]. Moreover, in a previous study, it was found that NMR parameters calculated at the B3LYP and B3PW91 levels were in good agreement [21]. Therefore, all of the calculations were done at the B3LYP level. The calculated CS tensors in the principal axis system (PAS) with order $\sigma_{33} > \sigma_{22} > \sigma_{11}$ [23] were converted to measurable NMR parameters, i.e., the isotropic (CSI) and anisotropic chemical shielding CS (CS^A) parameters, using Eqs. (1) and (2) [7]; the NMR parameters of ^{29}Si, ^{11}B, and ^{31}P atoms for the investigated (6,0) *zigzag* single-walled BPNT models are summarized in Table 2.

$$CS^I(\text{ppm}) = 1/3(\sigma_{11} + \sigma_{22} + \sigma_{33}), \quad (1)$$

$$CS^A(\text{ppm}) = \sigma_{33} - 1/2(\sigma_{11} + \sigma_{22}). \quad (2)$$

For NQR parameters, computational calculations do not directly return experimentally measurable NQR parameters, i.e., the nuclear quadrupole coupling constant (C_Q) and asymmetry parameter (η_Q). Therefore, Eqs. (3) and (4) were used to calculate the EFG tensors to their proportional experimental parameters; C_Q is the interaction energy of the nuclear electric quadrupole moment (eQ) with the EFG tensors (electric field gradient) at the sites of quadrupole nuclei, but the asymmetry parameter (η_Q) is a quantity of the EFG tensors that describes the deviation from tubular symmetry at the sites of quadrupole nuclei. Nuclei with $I > 1/2$ (where I is the nuclear spin angular momentum) are active in NQR spectroscopy. The calculated EFG tensor eigenvalues in the principal axis system (PAS) with order $|q_{zz}| > |q_{yy}| > |qxx|$ were converted to measurable NQR parameters, i.e., the nuclear quadrupole coupling constant (C_Q) and asymmetry parameter (η_Q), using Eqs. (3) and (4). The standard Q values [$Q(^{11}B) = 40.59$ mb] reported by Pyykkö [24] are used in Eq. (3). The NQR parameters of ^{11}B nuclei for the investigated models of the (6,0) *zigzag* single-walled BPNTs are summarized in Table 3. All calculations were carried out by using the Gaussian 03 suite of programs [25].

$$C_Q(\mathrm{MHz}) = e^2 Q\ \mathrm{q}_{zz} h^{-1}, \quad (3)$$

$$\eta_Q = |(\mathrm{q}_{xx} - \mathrm{q}_{yy})/\mathrm{q}_{zz}| \quad 0 < \eta_Q < 1. \quad (4)$$

References

1. Ijima S (1991) Nature 354:56
2. Derycke V, Martel R, Appenzeller J, Avouris P (2002) Appl Phys Lett 80:2773
3. Liu C, Fan YY, Liu M, Cong HT, Cheng HM, Dresselhaus MS (1999) Science 286:1127
4. Zurek B, Autschbach J (2004) J Am Chem Soc 126:13079
5. Nojeh A, Lakatos GW, Peng S, Cho K, Pease RFW (2003) Nano Lett 3:1187
6. Mirzaei M, Mirzaei M (2010) Monatsh Chem 141:491
7. Mirzaei M, Seif A, Hadipour NL (2008) Chem Phys Lett 461:246
8. Moradian R, Azadi S, Vasheghani Farahani S (2008) Phys Lett A 372:6935
9. Qian Z, Hou S, Zhang J, Li R, Shen Z, Zhao X, Xue Z (2005) Physica E 30:81
10. Mirzaei M, Giahi M (2010) Physica E 42:1667
11. Mirzaei M, Mirzaei M (2010) J Mol Struct (Theochem) 951:69
12. Wu Q, Hu Z, Liu C, Wang X, Chen Y (2005) J Phys Chem B 109:19719
13. Roy S, Springborg M (2009) J Phys Chem C 113:81
14. Zhang SL (2001) Phys Lett A 285:207
15. Mirzaei M (2009) Physica E 41:883
16. Mirzaei M (2009) Z Phys Chem 223:815
17. Bovey FA (1988) Nuclear magnetic resonance spectroscopy. Academic, San Diego
18. Baei MT, Moradi AV, Moghimi M, Torabi P (2011) J Comput Chem. 967:179–184. doi:10.1016/j.comptc.2011.04.015
19. Hou S, Shen Z, Zhang J, Zhao X, Xue Z (2004) Chem Phys Lett 393:179
20. Bengu E, Marks LD (2001) Phys Rev Lett 86:2385
21. Mirzaei M, Hadipour NL (2006) J Phys Chem A 110:4833
22. Mothana B, Ban F, Boyd RJ (2005) Chem Phys Lett 401:7
23. Drago RS (1992) Physical Methods for Chemists, 2nd ed. Saunders College Publishing, Florida
24. Pyykkö P (2001) Mol Phys 99:1617
25. Frisch MJ, Trucks GW, Schlegel HB, Scuseria GE, Robb MA, Cheeseman JR, Zakrzewski VG, Montgomery JA Jr, Stratmann RE, Burant JC, Dapprich S, Millam JM, Daniels AD, Kudin KN, Strain MC, Farkas O, Tomasi J, Barone V, Cossi M, Cammi R, Mennucci B, Pomelli C, Adamo C, Clifford S, Ochterski J, Petersson GA, Ayala PY, Cui Q, Morokuma K, Malick DK, Rabuck AD, Raghavachari K, Foresman JB, Cioslowski J, Ortiz JV, Baboul AG, Stefanov BB, Liu G, Liashenko A, Piskorz P, Komaromi I, Gomperts R, Martin RL, Fox DJ, Keith T, Al-Laham MA, Peng CY, Nanayakkara A, Gonzalez C, Challacombe M, Gill PMW, Johnson B, Chen W, Wong MW, Andres JL, Gonzalez C, Head-Gordon M, Replogle ES, Pople JA (2003) Gaussian 03, revision B03. Gaussian Inc., Pittsburgh